(148) R. Copeland, letter to Edmond & Spark, ROE A29.191, 289, 1887 Jan 27.
(149) R. Copeland, letter to Mitchell, ROE A28.189, 38, 1880 Oct 11.
(150) R. Copeland, *Catalogue of the Crawford Library of the Royal Observatory Edinburgh*, by authority of Her Majesty's Government, 1890.
(151) R. Copeland, letter to Knobel, ROE A29.191, 369, 1887 Mar 24.
(152) R. Copeland, *MN*, **48**, 48, 1887.
(153) R. Copeland, letter to S. Perry, ROE A29.191, 391, 1887 Apr 9.
(154) R. Copeland, letter to Bredichin, ROE A29.191, 495, 1887 June 21.
(155) R. Copeland, letters to McLaren, ROE A29.191, 9 & 31, 1886 Jan 16 & 27.
(156) R. Copeland, letter to McLaren, ROE A29.191, 633, 1888 Jan 28.
(157) R. Copeland, in *Equatorial Book 2*, ROE A17.95 entries for 1889 June 8 & 17.
(158) R. Copeland, letters to Tarrant, ROE A29.191, 754 & 759, 1888 Sep 24 & Oct 18.
(159) R. Copeland, letters to Tweedale, ROE A29.191, 161 & 165, 1888 Oct 4 & 5.
(160) R. Copeland, letters to Clerke, ROE A29.191, 268, 1887 Jan 13.
(161) R. Copeland, letters to Espin, ROE A29.191, 208 & 212, 1886 Nov 26 & 27.
(162) R. Copeland, letters to Espin, ROE A29.191, 745 & 748, 1888 Aug 23 & 27.

REDISCUSSION OF ECLIPSING BINARIES. PAPER 17: THE F-TYPE TWIN SYSTEM CW ERIDANI

By Stephen Overall and John Southworth

Astrophysics Group, Keele University

CW Eri is a detached eclipsing binary system of two F-type stars with an orbital period of 2·728 d. Light-curves from two sectors of observations with the *Transiting Exoplanet Survey Satellite* (*TESS*) and previously published radial-velocity data are analysed to determine the system's physical properties to high precision. We find the masses of the two stars to be $1{\cdot}568 \pm 0{\cdot}016\ M_{\odot}$ and $1{\cdot}314 \pm 0{\cdot}010\ M_{\odot}$, the radii to be $2{\cdot}105 \pm 0{\cdot}007\ R_{\odot}$ and $1{\cdot}481 \pm 0{\cdot}005\ R_{\odot}$ and the system's orbit to have an eccentricity of $0{\cdot}0131 \pm 0{\cdot}0007$. The quality of the *TESS* photometry allows the definition of a new high-precision orbital ephemeris; however, no evidence of pulsation is found. We derive a distance to the system of $191{\cdot}7 \pm 3{\cdot}8$ pc, a value consistent with the *Gaia* DR3 parallax which yields a distance of $187{\cdot}9^{+0{\cdot}6}_{-0{\cdot}9}$ pc. The measured parameters of both stellar components are found to be in agreement with theoretical predictions for a solar chemical composition and an age of 1·7 Gyr.

Introduction

Detached eclipsing binaries (dEBs) are a vital source of stellar parameters as they allow direct measurement of the component stars' physical properties when combining light-curves and radial-velocity (RV) observations[1–3]. Detached systems are particularly useful as, in the absence of mass transfer, the components are representative of single stars and are therefore an invaluable source of data for testing and refining stellar-evolution models[4,5].

The volume and quality of light-curve data has increased enormously in recent years[6], especially from space-based exoplanet surveys such as *CoRoT*[7] and NASA's *Kepler*[8], *K2*[9], and *TESS*[10] (*Transiting Exoplanet Survey Satellite*) missions. This work is one of a series where we revisit known dEBs in order to refine their characterization with the benefit of this new era of photometry. Here we analyse CW Eridani using *TESS* light-curves alongside previously published RV data.

The dEB CW Eridani

HD 19115 was categorized as photometrically variable in 1967 by Strohmeier & Ott[11]. Popper[12] reported that the spectrum was double-lined and it was given the designation CW Eri by Kukarkin *et al.*[13]. Chen[14] reported on *UBV* photometric observations made at the Rosemary Hill Observatory between 1970 and 1972, publishing an ephemeris and relative sizes for the components. Further photometric observations were made by Mauder & Ammann[15] and, with the addition of spectroscopic observations made available to them by Popper, they recorded masses and radii for both components to 2–3% confidence and assigned a spectral type of F0.

Popper & Dumont[16] included CW Eri in their programme of *UBV* photometric observations at the Palomar and Kitt Peak observatories with the *B*- and *V*-band magnitudes given in Table I being recorded over 11 nights. Brancewicz & Dworak[17] included it in their catalogue of eclipsing binaries where they used numerical methods to characterize the system, giving a spectral type of F0+ and physical parameters to ~5% confidence.

TABLE I

Basic information on CW Eri.

Property	*Value*	*Reference*
Right ascension (J2000)	$03^h03^m59^s.95$	22
Declination (J2000)	$-17°44'16''.06$	22
Henry Draper designation	HD 19915	23
Hipparcos designation	HIP 14273	24
Tycho designation	TYC 5868-881-1	25
Gaia DR3 designation	5152756553745197952	22
Gaia DR3 parallax	5·2380 ± 0·0198 mas	22
TESS Input Catalog designation	TIC 98853987	26
B magnitude	8·79 ± 0·07	16
V magnitude	8·43 ± 0·07	16
G magnitude	8·306 ± 0·003	22
J magnitude	7·799 ± 0·020	27
H magnitude	7·659 ± 0·034	27
K_s magnitude	7·626 ± 0·023	27
Spectral type	F2 V	28

The most complete investigations were carried out by Popper[12,18] based on spectrograms taken at the Lick Observatory between 1967 and 1974 along with photometry from Chen[14] and Mauder & Ammann[15]. Popper determined the spectral types of the components as F1 and F4, gave their masses to 2% confidence, and determined their radii to 2·5% and 4·5% for the primary and secondary components, respectively.

Outside automated surveys, in the years since Popper few observations have been made. Wolf & Kern[19] recorded three observations as part of their photometric survey of the southern hemisphere, giving a *V*-band magnitude

ranging from 8·39 at quadrature to 8·90 during primary eclipse. Perry & Christodoulou[20] included it in their *uvbyβ* interstellar-reddening survey of the southern hemisphere. Nordström *et al.*[21] made three spectroscopic observations as part of their RV survey of early F-type dwarfs.

Table I shows basic information for CW Eri. The B and V magnitudes are those recorded by Popper & Dumont[16]. These were explicitly based on observations made outside of an eclipse and have since been widely used. The J, H, and K_s magnitudes are those reported by 2MASS from observations made at JD 2451052·9027±30 sec. At this time the system will have been within a secondary eclipse so these will be below the system's maximum brightness. The spectral type of F2 V is given by Houk & Smith-Moore[28] as part of the *Michigan Catalogue of HD Stars*, Vol 4.

Observational material

CW Eri was observed twice by the *TESS* mission[10], first in sector 4 from 2018/10/19 to 2018/11/14 and again in sector 31 from 2020/10/22 to 2020/11/18, each in short-cadence mode with a 120-s sampling rate. Both sectors show light-curves covering a period of approximately 25 days with a break near the midpoint for data download. Unambiguous primary and secondary eclipses are seen in addition to a sinusoidal variation resulting from the ellipsoidal effect (Fig. 1).

The *TESS* time-series data for the two sectors were downloaded from the MAST archive* and subsequently processed using the LIGHTKURVE[29] and ASTROPY[30] Python packages. These data consist of simple aperture photometry (SAP) and pre-search data conditioning SAP (PDCSAP) flux measurements[31]. We based our analysis on the SAP data as they are well-behaved whereas extraneous variability was seen in the PDCSAP data from sector 4. Data points with no flux value recorded (NaN) and those with a non-zero QUALITY flag were cut, as were those within a distorted secondary eclipse within sector 4 from BJD 2458420·0 to 2458423·0. A total of 13841 data points from sector 4 and 16671 from sector 31 were considered for subsequent analysis.

The *Gaia* DR3 database† was queried for potential sources of third light within 2 arcmin of CW Eri. Six of the seven objects found are at least 10 mag fainter than CW Eri in the G-band so contribute negligible light. The remaining object, TYC 5868-428-1, has a G-band magnitude of 11·053 mag with the resulting flux ratio of 0·080 being adopted as the initial value of the fitted third-light parameter in the following analysis.

Light-curve analysis

The remaining SAP flux data were converted to magnitudes then rectified to zero and detrended by fitting and subtracting a quadratic polynomial across the whole of each sector. This was refined after initial attempts at fitting, with the best results achieved by subtracting a second quadratic fit from those data in sector 4 following the mid-sector break. The resulting light-curves, shown in Fig. 1, consist of four isolated half-sectors over a time interval of ~759 d. We adopt the standard definition of the primary eclipse as being the deeper of the two which occurs when the larger and brighter component, which we label star A, is eclipsed by the smaller star B.

* Mikulski Archive for Space Telescopes, https://mast.stsci.edu/portal/Mashup/Clients/Mast/Portal.html

†https://vizier.cds.unistra.fr/viz-bin/VizieR-3?-source=I/355/gaiadr3

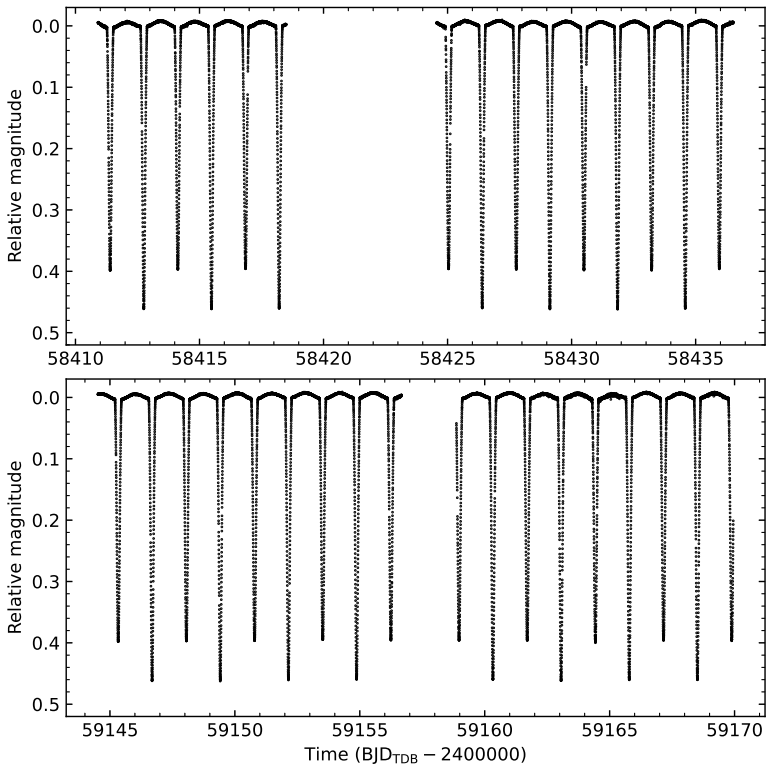

FIG. 1

TESS short-cadence SAP photometry of CW Eri from sectors 4 (top) and 31 (bottom). The flux measurements have been converted to magnitude units then rectified to zero magnitude by the subtraction of low-order polynomials.

The data were fitted using version 43 of the JKTEBOP* code[32,33] with a total 30 512 data points fitted as the four separate half-sectors. Each light-curve was fitted for the orbital period (P) and the time of mid-primary eclipse (T_0) with our reference time being the primary eclipse closest to the midpoint of the data. Also fitted were the sum ($r_A + r_B$) and ratio ($k = r_B/r_A$) of the fractional radii, the orbital inclination (i), the orbital eccentricity (e) and argument of periastron (ω) through the Poincaré elements $e \cos \omega$ and $e \sin \omega$, the stars' central-surface-brightness ratio (γ), the amount of third light ($L3$), and each star's reflected light.

We adopted the power-2 limb darkening (LD) law with *TESS*-specific coefficients taken from Claret & Southworth[34]. The coefficients were interpolated for star A ($T_{eff} = 6840$ K and $\log g = 4{\cdot}0$) and star B ($T_{eff} = 6560$ K and $\log g = 4{\cdot}2$), each with a solar metallicity ([Fe/H] = 0·0). For both stars, the scaling coefficient c was left free to fit and α was fixed.

*http://www.astro.keele.ac.uk/jkt/codes/jktebop.html

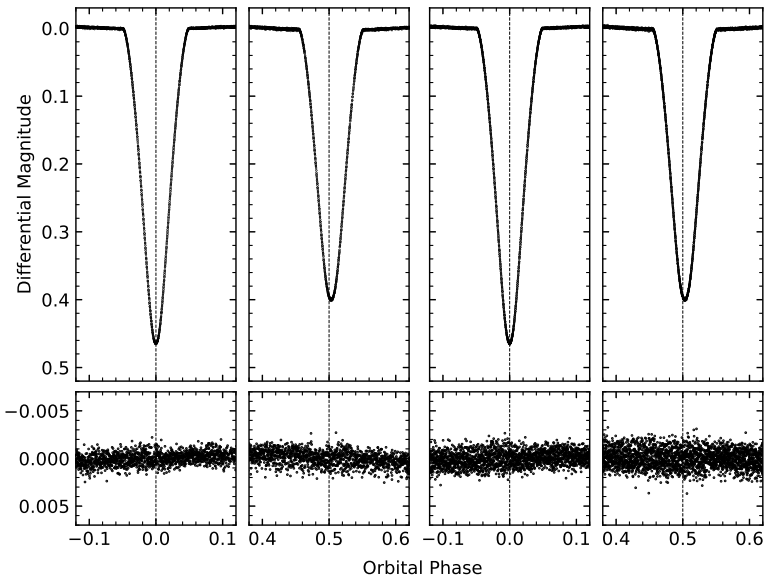

FIG. 2

Best fit to the full *TESS* sector-4 light-curve of CW Eri using JKTEBOP. The primary and secondary eclipse of the first half-sector are shown to the left and those for the second half-sector to the right. The residuals are shown on an enlarged scale in the lower panels.

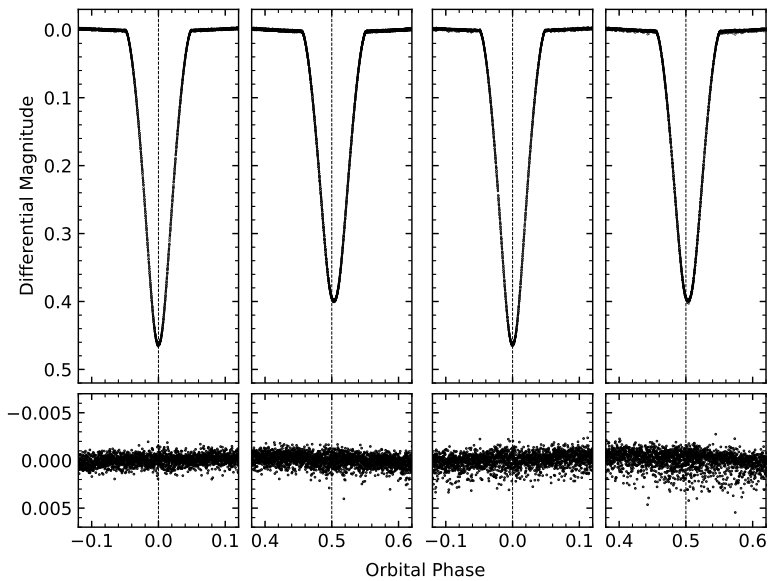

FIG. 3

Same as Fig. 2 but for *TESS* data from sector 31.

The best fits to the light-curves are shown in Figs. 2 and 3 where it can be seen that the secondary eclipse is slightly offset from phase 0·50, confirming a small orbital eccentricity. As F-type stars may exhibit γ Doradus or δ Scuti pulsations[35] the residuals of the fits were analysed with Lomb–Scargle periodograms, but no evidence of pulsation was found.

The final values and uncertainties for the fitted parameters of each half-sector were separately determined with 10 000 Monte Carlo (MC) simulations[32] and a residual permutation (RP) algorithm[36], as implemented by JKTEBOP tasks 8 and 9, respectively. The latter method successively shifts the best-fit residuals along the light-curve until they are cycled back to their initial position. With each shift a new fit is made and the final distribution of each fitted parameter gives an estimate of its uncertainty. While the MC simulations are sensitive to Poisson noise, the RP algorithm is additionally sensitive to correlated noise[36]. The fitted parameters for each half-sector are given in Table II with the uncertainties being the 1σ values of either the MC or RP simulations. The selection of uncertainties for each parameter is based on the method which yields the larger weighted mean error bar. The adopted parameters for CW Eri, as given in Table III, are the weighted mean and uncertainty of the corresponding fitted parameters across the four half-sectors.

Orbital ephemeris

With the light-curve analysis yielding consistent orbital parameters, we sought to derive a high-precision orbital ephemeris for the system. In order to base this on the longest possible dataset, historical minima-timing data for CW Eri were obtained from the TIming DAtabase at Krakow (TIDAK) team[37]. While the majority of minima timings were given without an uncertainty, all included a weight value between 1 and 10. Where missing, estimated uncertainties were generated by scaling a base estimate of 0·004 by the reciprocal of the observation's weight. To these data were added the primary epoch and period from fitting each of the four half-sectors of *TESS* data with their uncertainties scaled up by a factor of 5 to cover any scatter.

The existing TIDAK ephemeris* was used to calculate cycle numbers and assign minima types (primary or secondary) to the eclipses after which linear, quadratic, and cubic polynomials were fitted to reveal trends in the timings. Initial attempts at fitting the data revealed excessive scatter from a number of sources and the final fitted ephemeris is based only on the *TESS* observations and those from TIDAK with a weight of 10. With the fitting complete the quadratic and cubic fits were discounted, as they were poorly constrained by the data, and the following linear ephemeris was adopted:

$$\text{Min I} = \text{BJD}_{\text{TDB}}\ 2452500{\cdot}37624(69) + 2{\cdot}72837024(27)E \qquad (1)$$

with E being the cycle number since the reference time and the bracketed values being the uncertainties in the last digit of the preceding values. The final eclipse timing data used in this analysis are given in Table IV and the residuals of the linear fit are shown in Fig. 4.

Radial velocities

The RV measurements originally published by Popper[12] were reanalysed. The observations were made between 1967 and 1974 at the Lick Observatory and consist of 38 RVs for star A and 35 for star B. Popper's data gives RVs to

*https://www.as.up.krakow.pl/minicalc/ERICW.HTM

TABLE II

The fitted parameters of CW Eri for each of the four TESS half-sector light-curves using the JKTEBOP code. The uncertainties are 1σ values derived from either Monte Carlo or residual-permutation simulations. For each parameter the uncertainties given are from the method yielding the larger weighted mean uncertainty across the half-sectors. A value of 2400 000 has been subtracted from the eclipse times to save space.

Parameter	*Sector 4.1*	*Sector 4.2*	*Sector 31.1*	*Sector 31.2*
Fitted parameters:				
Primary eclipse time (BJD_{TDB})	58415·482929 ± 0·000022	58431·853144 ± 0·000015	59152·142894 ± 0·000015	59163·056373 ± 0·000020
Orbital period (d)	2·7283891 ± 0·0000157	2·7283696 ± 0·0000092	2·7283737 ± 0·0000065	2·7283805 ± 0·0000117
Orbital inclination (°)	86·366 ± 0·037	86·373 ± 0·033	86·412 ± 0·022	86·313 ± 0·040
Sum of the fractional radii	0·30659 ± 0·00021	0·30676 ± 0·00019	0·30651 ± 0·00013	0·30682 ± 0·00023
Ratio of the radii	0·7042 ± 0·0017	0·7033 ± 0·0011	0·7048 ± 0·0010	0·7026 ± 0·0012
Central-surface-brightness ratio	0·9262 ± 0·0065	0·9203 ± 0·0061	0·9309 ± 0·0041	0·9203 ± 0·0068
Third light	−0·0025 ± 0·0019	−0·0014 ± 0·0017	0·0024 ± 0·0012	−0·0036 ± 0·0021
LD c coefficient of star A	0·592 ± 0·027	0·622 ± 0·025	0·573 ± 0·017	0·611 ± 0·028
LD c coefficient of star B	0·614 ± 0·019	0·601 ± 0·018	0·620 ± 0·012	0·608 ± 0·021
LD α coefficient of star A		0·4676 (fixed)		
LD α coefficient of star B		0·4967 (fixed)		
$e \cos \omega$	0·00492 ± 0·00002	0·00491 ± 0·00001	0·00513 ± 0·00001	0·00513 ± 0·00002
$e \sin \omega$	−0·01181 ± 0·00108	−0·01290 ± 0·00069	−0·01135 ± 0·00066	−0·01229 ± 0·00082
Derived parameters:				
Fractional radius of star A	0·17990 ± 0·00026	0·18010 ± 0·00017	0·17979 ± 0·00016	0·18021 ± 0·00018
Fractional radius of star B	0·12669 ± 0·00016	0·12666 ± 0·00011	0·12672 ± 0·00010	0·12661 ± 0·00012
Orbital eccentricity	0·01279 ± 0·00099	0·01381 ± 0·00064	0·01245 ± 0·00060	0·01332 ± 0·00075
Light ratio ℓ_B/ℓ_A	0·4535 ± 0·0014	0·4537 ± 0·0010	0·4542 ± 0·0009	0·4510 ± 0·0010

TABLE III

The adopted parameters of CW Eri derived from the four TESS half-sector light-curves fitted with the JKTEBOP code. Other than the time of primary eclipse each is the weighted mean of the corresponding fitted parameter values and 1σ uncertainties for each fitted half-sector given in Table II.

Parameter	*Value*
Fitted parameters:	
Time of primary eclipse (BJD_{TDB})	2458415·482929 ± 0·000022
Orbital period (d)	2·7283751 ± 0·0000068
Orbital inclination (°)	86·381 ± 0·042
Sum of the fractional radii	0·30662 ± 0·00015
Ratio of the radii	0·7037 ± 0·0011
Central-surface-brightness ratio	0·9262 ± 0·0057
Third light	−0·0002 ± 0·0030
LD c coefficient of star A	0·593 ± 0·024
LD c coefficient of star B	0·613 ± 0·009
LD α coefficient of star A	0·4676 (fixed)
LD α coefficient of star B	0·4967 (fixed)
$e \cos \omega$	0·00502 ± 0·00013
$e \sin \omega$	−0·01210 ± 0·00076
Derived parameters:	
Fractional radius of star A	0·18000 ± 0·00020
Fractional radius of star B	0·12667 ± 0·00005
Orbital eccentricity	0·01310 ± 0·00067
Light ratio ℓ_B/ℓ_A	0·4532 ± 0·0015

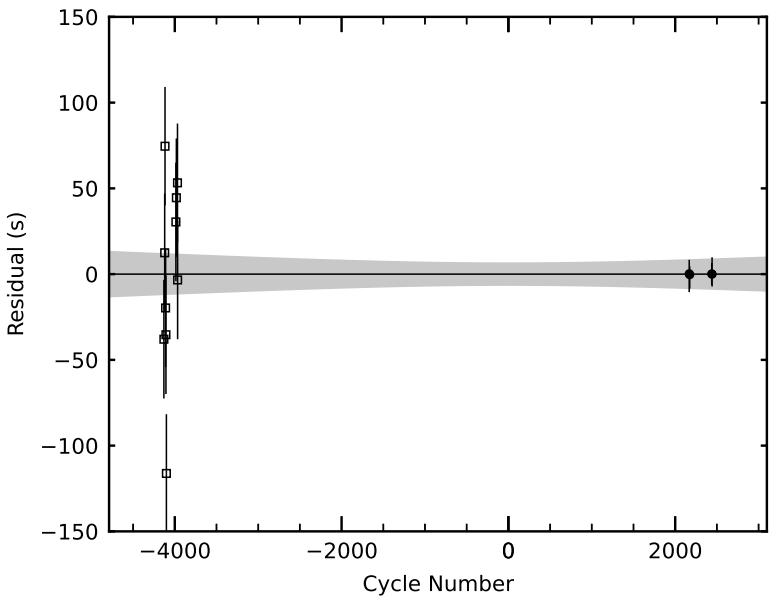

FIG. 4

Observed minus calculated ($O-C$) diagram of the times of primary minimum *versus* the fitted linear ephemeris. Timings from the *TESS* data are shown with with filled circles and those from the literature are shown as open squares where uncertainties have been estimated. The shaded areas indicate the 1σ uncertainty in the ephemeris determined from these data.

TABLE IV

Times of published mid-eclipse for CW Eri and their residuals versus the fitted ephemeris.

Orbital cycle	*Eclipse time* (BJD_{TDB})	*Uncertainty* (*d*)	*Residual* (*d*)	*Reference*
−4130·5	2441230·842503	0·000400	−0·000439	14
−4121·0	2441256·762604	0·000400	0·000144	14
−4117·0	2441267·676804	0·000400	0·000863	14
−4110·0	2441286·774304	0·000400	−0·000228	14
−4106·0	2441297·687604	0·000400	−0·000409	14
−4100·5	2441312·692704	0·000400	−0·001345	14
−3986·5	2441623·728610	0·000400	0·000352	14
−3981·0	2441638·734809	0·000400	0·000515	14
−3967·5	2441675·567908	0·000400	0·000616	14
−3966·0	2441679·659808	0·000400	−0·000039	14
2168·0	2458415·482929	0·000109	0·000003	This work
2174·0	2458431·853144	0·000075	−0·000004	This work
2438·0	2459152·142894	0·000074	0·000002	This work
2442·0	2459163·056373	0·000099	−0·000000	This work

one decimal place and HJD time-stamps to three decimal places and, in the absence of uncertainties, we applied equal weighting to all measurements. The RVs were analysed with JKTEBOP based on the ephemeris and orbital parameters derived from the photometric fitting with the uncertainties of the fitted results determined using Monte Carlo simulations (see Paper VI, ref. 38).

Initial fitting was carried out with fixed values for T_0 and P which yielded results very similar to Popper's with slightly worse r.m.s. residuals for star B. Given the low temporal resolution of the observations, we investigated whether allowing these parameters to be varied when fitting the RV orbits would yield an improved fit. It was found that allowing T_0 to vary yielded a demonstrable improvement in the fitted RV orbits with lower uncertainties and r.m.s. residuals; these are the results reported here.

The fitted orbits are shown in Fig. 5. Parameters for the spectroscopic orbits are given in Table V which shows them to be in good agreement with Popper[12] while having lower uncertainties and residuals. Nordström *et al.*[21] give only an overall systemic velocity of $V_\gamma = 37{\cdot}16 \pm 2{\cdot}94$ km s^{-1}, based on three observations, which also agrees well with our findings. Few works have published any further RV data on CW Eri, with Duflot *et al.*[39] giving $V_\gamma = 36{\cdot}4$ km s^{-1} in their Wilson-Evans-Batten catalogue and Gontcherov[40] giving a value $V_\gamma = 36{\cdot}8 \pm 2{\cdot}1$ km s^{-1}, potentially based on the values published by Nordström and Duflot, with both showing some overlap with our individual RVs.

TABLE V

Spectroscopic orbits for CW Eri from the literature and from the reanalysis of the RVs in the current work. All quantities are in km s^{-1}.

Source	K_A	K_B	$V\gamma_{,A}$	$V\gamma_{,B}$	*r.m.s residual*
Popper[12]	98·9	118·0	36·4	35·7	1·70, 2·80
	±0·3	±0·6	±0·3	±0·5	
This work	98·7	117·7	36·1	36·2	1·55, 2·55
	±0·3	±0·5	±0·3	±0·4	

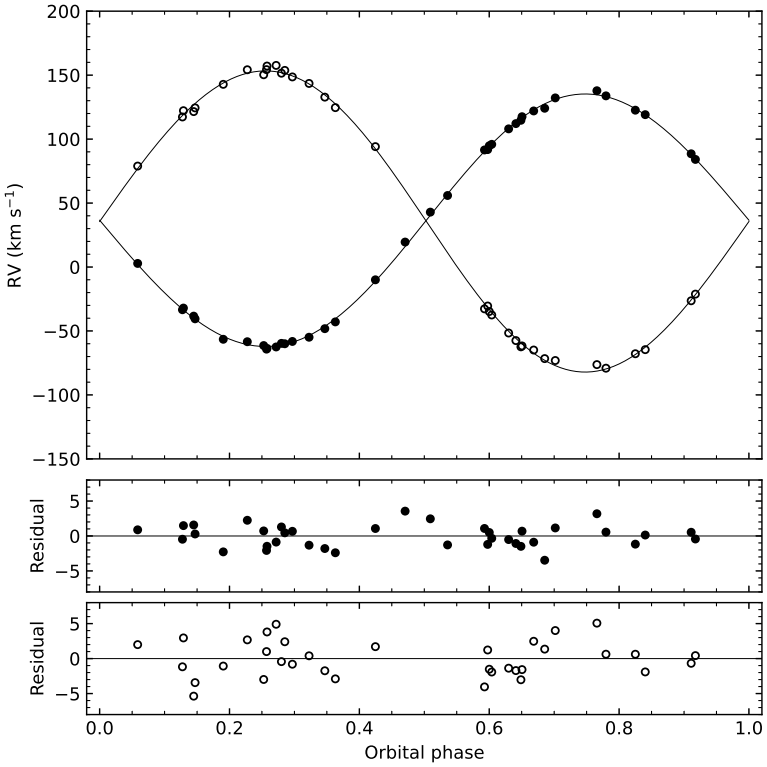

FIG. 5

RVs of CW Eri measured by Popper[12] (filled circles for star A and open circles for star B) compared to the best-fitting spectroscopic orbits from JKTEBOP (solid curves). The residuals are given in the lower panels separately for the two components.

Physical properties of CW Eri

The physical properties of CW Eri were calculated based on the parameters derived from the light-curves (Table III), the RV fitting (Table V), and the new ephemeris calculated above. The uncertainties for r_A and r_B were increased to 0·2% following the recommendation from Maxted *et al.*[41]. Effective temperature values were taken from Popper[12] where a value for both components has been given with accompanying uncertainty. The JKTABSDIM code[42] was used to calculate the system's properties given in Table VI with uncertainties propagated using a perturbation approach. Standard formulae[43] and the reference solar values from the IAU[44] were used.

The results show that the masses and radii are determined to a precision of better than 1·0%, meeting the criteria for inclusion in the *Detached Eclipsing Binary Catalogue* (*DEBCat*⋆, ref. 3). The mass measurements are in agreement with the original values published by Popper[12], as expected as they are based

⋆https://www.astro.keele.ac.uk/jkt/debcat/

TABLE VI

Physical properties of CW Eri defined using the nominal solar units given by IAU 2015 Resolution B3 (ref. 44).

Parameter	*Star A*	*Star B*
Mass ratio	0·8385 ± 0·0047	
Semi-major axis of relative orbit ($R_\odot^N$)	11·694 ± 0·034	
Mass ($M_\odot^N$)	1·568 ± 0·016	1·314 ± 0·010
Radius ($R_\odot^N$)	2·1048 ± 0·0074	1·4812 ± 0·0052
Surface gravity (log[cgs])	3·9869 ± 0·0026	4·2156 ± 0·0022
Density ($\rho_\odot$)	0·1681 ± 0·0011	0·4045 ± 0·0027
Effective temperature (K)	6839 ± 87	6561 ± 98
Luminosity log($L/L_\odot^N$)	0·941 ± 0·022	0·564 ± 0·026
M_{bol} (mag)	2·387 ± 0·056	3·330 ± 0·065
Distance (pc)	191·7 ± 3·8	

on the same RV data. The measured radii are consistent with those from Popper (2·08±0·05 and 1·56±0·07 $R_\odot$) but are much more precise due to the availability of the *TESS* photometry.

We determined the distance to the system based on the *B* and *V* apparent magnitudes from Popper & Dumont[16] and those in the *J*, *H*, and K_s-bands from 2MASS[27] (Table I). The 2MASS magnitudes are based on observations made during a secondary eclipse which were corrected for by subtracting the fitted light-curve model at the corresponding phase to find revised values of $J = 7{\cdot}658 \pm 0{\cdot}022$, $H = 7{\cdot}518 \pm 0{\cdot}035$, and $K_s = 7{\cdot}485 \pm 0{\cdot}025$ mag. We searched for reliable observations made in the Cousins *R* and *I* bands but found none. An interstellar extinction value of $E(B–V) = 0{\cdot}013 \pm 0{\cdot}015$ was adopted from the STILISM tool* and bolometric corrections from Girardi *et al.*[45] were used.

The *Gaia* DR3[22] parallax yields a distance of $187{\cdot}9^{+2{\cdot}6}_{-2{\cdot}9}$ pc for CW Eri, with the renormalized unit weight error (RUWE) of 1·029 indicating a reliable astrometric solution. This is in agreement with distances based on the bolometric corrections of Girardi *et al.*[45] when applied to the *B*, *V*, and *J*-band magnitudes, with the *J*-band yielding the best match at 188·4±3·0 pc. A similar pattern is seen when using the passband-specific surface brightness–T_{eff} relations of Kervella *et al.*[46]. Both methods yield slightly larger distances than *Gaia* using the *H* and K_s-band magnitudes; however, the weighted mean of all of the derived distances is 191·7±3·8 pc which is in agreement with the *Gaia* value.

Comparison with theoretical models

To test our results, the measured properties of the components of CW Eri were compared with predictions of PARSEC theoretical stellar-evolutionary models[47] in plots of mass *versus* radius, T_{eff}, and luminosity. The best agreement was found for models based on a solar composition (fractional metal abundance of $Z = 0{\cdot}017$) and an age of 1·7 Gyr. This gives a very good fit to star A with star B appearing slightly larger and more luminous than the model predictions. Choosing a model with lower metallicity gives a closer fit to star B's radius and luminosity but at the expense of star A which now appears slightly smaller and less massive than predicted, and both components are cooler than the model. The converse is found when higher-metallicity models are used with the T_{eff} being most sensitive to any change. Fig. 6 shows models ranging from slightly sub-solar ($Z = 0{\cdot}014$) through solar to slightly super-solar metal abundance ($Z = 0{\cdot}020$).

*https://stilism.obspm.fr

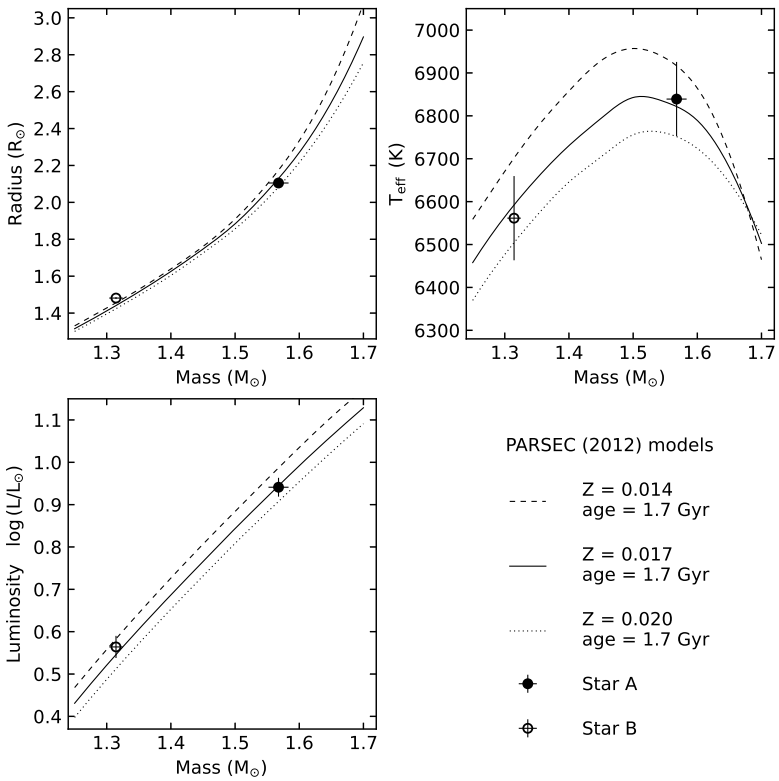

FIG. 6

Comparison between the theoretical predictions of PARSEC models[47] and the measured properties of CW Eri presented here for stellar mass *versus* radius, $T_{\rm eff}$, and luminosity. The ages and metal abundances of the chosen theoretical models are given in the legend within the lower right quadrant.

This choice of age and metallicity is further supported with a Hertzsprung–Russell diagram showing the evolutionary tracks of PARSEC model stars of $Z = 0{\cdot}017$ and masses 1·3, 1·45, and 1·6 $M_{\odot}$ (Fig. 7). Both components of CW Eri are consistent with model stars of similar mass which have evolved away from the ZAMS line into the upper half of the main sequence. Comparisons were also made with equivalent MIST[48,49] models and evolutionary tracks, with broadly similar results except that the star A is hotter than predicted.

While the chosen PARSEC model has a good fit to the mass, radius, and $T_{\rm eff}$ of the components, we note that the metallicity is in disagreement with published values. Perry & Christodoulou[20] give [Fe/H] = –0·32 in their *uvbyβ* survey of southern hemisphere A and F-type stars. A value of [Fe/H] = –0·39 was published in the *Geneva-Copenhagen Catalogue* by Holmberg *et al.*[50] and subsequently recalculated as –0·26 by Casagrande *et al.*[51]. A plausible answer to this discrepancy is that the metallicity was calculated assuming that the photometry of the system represents that of a single star rather than the combined light of two stars of different colours.

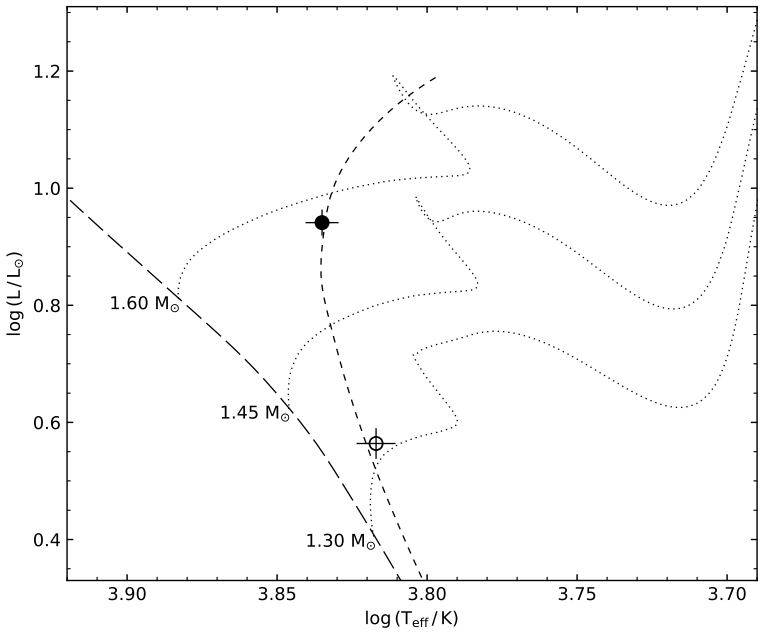

FIG. 7

Hertzsprung–Russell diagram showing the components of CW Eri (filled circle for star A and open circle for star B) and selected predictions from the PARSEC models[47] (dotted lines). The zero-age main sequence is shown with a long-dashed line, and an ioschrone for an age of 1·7 Gyr with a short-dashed line. Models for 1·30, 1·45, and 1·60 $M_{\odot}$ are shown (labelled) with a metal abundance of $Z = 0{\cdot}017$.

Summary

CW Eri is a dEB consisting of a pair of F-type stars that has remained largely ignored since it was last studied by Popper in 1983[12]. We have revisited the system, making use of two sectors of *TESS* photometry, and determined its photometric parameters to high precision. By combining these results with Popper's original RVs we refined the spectroscopic orbits and subsequently obtained high-quality measurements of the physical properties of the system. The residuals were analysed for evidence of pulsations with none being found. By combining eclipse timings from the four fitted *TESS* half-sectors with archival eclipse-timing data we defined a new high-precision orbital ephemeris.

The properties of both stars were found to be consistent with PARSEC models for a solar metallicity and an age of 1·7 Gyr. The evolutionary tracks show the stars to be in the second half of their main-sequence lifetime with the more massive star A having evolved farther from the ZAMS. With two stars of well-constrained properties and age this system lends itself to the calibration of future stellar models, a role which could be further enhanced by the analysis of follow-up spectroscopy to constrain their atmospheric characteristics better.

Acknowledgements

We gratefully acknowledge the financial support of the Science and Technologies Facilities Council (STFC) in the form of a PhD studentship. This paper includes data collected by the *TESS* mission and obtained from the MAST data archive at the Space Telescope Science Institute (STScI). Funding for the *TESS* mission is provided by NASA's Science Mission Directorate. STScI is operated by the Association of Universities for Research in Astronomy, Inc., under NASA contract NAS 5–26555. The following resources were used in the course of this work: the NASA Astrophysics Data System; the *Simbad* database operated at CDS, Strasbourg, France; and the arχiv scientific paper preprint service operated by Cornell University. Finally, we thank Jerzy Kreiner and Bartek Zakrzewski for providing TIDAK ephemeris data for CW Eri *via* private communication.

References

(1) J. Andersen, *A&ARv*, **3**, 91, 1991.
(2) G. Torres, J. Andersen & A. Giménez, *A&ARv*, **18**, 67, 2010.
(3) J. Southworth, in *Living Together: Planets, Host Stars and Binaries* (S. M. Rucinski, G. Torres & M. Zejda, eds.), 2015, *Astronomical Society of the Pacific Conference Series*, vol. 496, p. 321.
(4) A. Claret & G. Torres, *A&A*, **592**, A15, 2016.
(5) A. Tkachenko *et al.*, *A&A*, **637**, A60, 2020.
(6) J. Southworth, *Universe*, **7**, 369, 2021.
(7) M. Deleuil *et al.*, *A&A*, **619**, A97, 2018.
(8) W. J. Borucki, *Reports on Progress in Physics*, **79**, 036901, 2016.
(9) S. B. Howell *et al.*, *PASP*, **126**, 398, 2014.
(10) G. R. Ricker *et al.*, *Journal of Astronomical Telescopes, Instruments, and Systems*, **1**, 014003, 2015.
(11) W. Strohmeier & H. Ott, *IBVS*, **195**, 1, 1967.
(12) D. M. Popper, *AJ*, **88**, 1242, 1983.
(13) B. V. Kukarkin *et al.*, *IBVS*, **717**, 1, 1972.
(14) K. Y. Chen, *Acta Astron*, **25**, 89, 1975.
(15) H. Mauder & M. Ammann, *Mitteilungen der Astronomischen Gesellschaft Hamburg*, **38**, 231, 1976.
(16) D. M. Popper & P. J. Dumont, *AJ*, **82**, 216, 1977.
(17) H. K. Brancewicz & T. Z. Dworak, *Acta Astron*, **30**, 501, 1980.
(18) D. M. Popper, *ARA&A*, **18**, 115, 1980.
(19) G. W. Wolf & J. T. Kern, *ApJS*, **52**, 429, 1983.
(20) C. L. Perry & D. M. Christodoulou, *PASP*, **108**, 772, 1996.
(21) B. Nordström *et al.*, *A&AS*, **126**, 21, 1997.
(22) Gaia Collaboration *et al.*, *A&A*, **649**, A1, 2021.
(23) A. J. Cannon & E. C. Pickering, *Annals of Harvard College Observatory*, **95**, 1, 1920.
(24) ESA (ed.), *The Hipparcos and Tycho Catalogues*. ESA Special Publication, vol. 1200, 1997.
(25) E. Høg *et al.*, *A&A*, **355**, L27, 2000.
(26) K. G. Stassun *et al.*, *AJ*, **158**, 138, 2019.
(27) R. M. Cutri *et al.*, *2MASS All Sky Catalog of point sources*. (The IRSA 2MASS All-Sky Point Source Catalog, NASA/IPAC Infrared Science Archive., Caltech, US), 2003.
(28) N. Houk & M. Smith-Moore, *Michigan Catalogue of Two-dimensional Spectral Types for the HD Stars. Volume 4* (University of Michigan), 1988.
(29) Lightkurve Collaboration *et al.*, '(Lightkurve: Kepler and TESS Time Series Analysis in Python)', Astrophysics Source Code Library, 2018.
(30) Astropy Collaboration *et al.*, *ApJ*, **935**, 167, 2022.
(31) J. M. Jenkins *et al.*, in *Software and Cyberinfrastructure for Astronomy IV* (G. Chiozzi & J. C. Guzman, eds.), 2016, *Society of Photo-Optical Instrumentation Engineers* (*SPIE*) *Conference Series*, vol. 9913, p. 99133E.
(32) J. Southworth, P. F. L. Maxted & B. Smalley, *MNRAS*, **351**, 1277, 2004.
(33) J. Southworth, *A&A*, **557**, A119, 2013.
(34) A. Claret & J. Southworth, *A&A*, **664**, A128, 2022.
(35) K. Uytterhoeven *et al.*, *A&A*, **534**, A125, 2011.
(36) J. Southworth, *MNRAS*, **386**, 1644, 2008.
(37) J. M. Kreiner, *Acta Astron*, **54**, 207, 2004.

(38) J. Southworth, *The Observatory*, **141**, 234, 2021.
(39) M. Duflot, P. Figon & N. Meyssonnier, *A&AS*, **114**, 269, 1995.
(40) G. A. Gontcharov, *AL*, **32**, 759, 2006.
(41) P. F. L. Maxted *et al.*, *MNRAS*, **498**, 332, 2020.
(42) J. Southworth, P. F. L. Maxted & B. Smalley, *A&A*, **429**, 645, 2005.
(43) R. W. Hilditch, *An Introduction to Close Binary Stars* (Cambridge University Press), 2001.
(44) A. Prša *et al.*, *AJ*, **152**, 41, 2016.
(45) L. Girardi *et al.*, *A&A*, **391**, 195, 2002.
(46) P. Kervella *et al.*, *A&A*, **426**, 297, 2004.
(47) A. Bressan *et al.*, *MNRAS*, **427**, 127, 2012.
(48) A. Dotter, *ApJS*, **222**, 8, 2016.
(49) J. Choi *et al.*, *ApJ*, **823**, 102, 2016.
(50) J. Holmberg, B. Nordström & J. Andersen, *A&A*, **475**, 519, 2007.
(51) L. Casagrande *et al.*, *A&A*, **530**, A138, 2011.

CORRESPONDENCE

To the Editors of 'The Observatory'

Willem Henri Julius (1860–1925)

In her retrospective review[1] of Charles Abbot's 1911 book *The Sun*[2], Virginia Trimble notes that 'W. H. Julius' is mentioned and wonders who he was and what his contributions to solar physics were. Andrew Young has already briefly outlined Julius' contributions[3] but I have unearthed a few more details which I thought might also be of interest. As Prof. Trimble notes, Julius is not included in the *Biographical Encyclopedia of Astronomers*[4], at least in the edition to which I have access. However, Brüggenthies & Dick's *Biographical Index of Astronomy*[5] does have an entry for one 'Julius, Willem Henri' which gives further entries in the *Dictionary of Scientific Biography* (*DSB*; by Marcel Minnaert)[6] and the on-line *Finding List of Obituary Notes of Astronomers*[7] (*ONA*) compiled by Duerbeck, Ott & Dick. The *ONA*, in turn, gives three obituaries, of which I was able to locate two[8,9], including one in this *Magazine*. A further search of the NASA ADS Bibliographical Database for items about Julius published in the years shortly after his death found one by Einstein that appeared in *ApJ*[10]. It is not a conventional obituary but a recap of some of Julius' ideas and an appeal that they not be overlooked.

The two obituaries[8,9] are both anonymous, single, short paragraphs and do little more than note Julius' death. Most of what follows is based on the entry by Minnaert in the *DSB* and Einstein's paper in *ApJ*. Minnaert was Julius' research student[11] and later occupied the Chair that Julius had held (though Minnaert was not the immediate successor). Einstein was a long-standing friend.

Willem Henri Julius (his forenames were sometimes Anglicised to William Henry; Fig. 1) was born in Utrecht on 1860 August 4. He enrolled at the University of Utrecht in 1879, where he studied mathematics and physics, gaining a doctorate under the supervision of Buys Ballot. (Christophorus Buys Ballot, 1817–90, is primarily remembered as a meteorologist, but at the time he supervised Julius he held Chairs in Physics and Mathematics, having initially been appointed to teach Mineralogy and Geology and then holding a Chair